Factors Affecting Electroplated Semiconductor Material Properties: The Case Study of Deposition Temperature on Cadmium Telluride

A.A. Ojo[1,2]* and I.M. Dharmadasa[2]

[1]Department of Mechanical Engineering, Ekiti State University (EKSU), Ado-Ekiti, Nigeria.
[2]Electronic Materials and Sensors Group, Materials and Engineering Research Institute (MERI), Sheffield Hallam University, Sheffield S1 1WB, UK

Abstract

Electrodeposition of cadmium telluride (CdTe) on fluorine doped tin oxide (FTO) using two electrode configuration was successfully achieved with the main focus on the growth temperature. The electroplating temperatures explored ranges between (55 and 85)°C for aqueous electrolytes containing 1.5 M cadmium nitrate tetrahydrate $(Cd(NO_3)_2 \cdot 4H_2O)$ and 0.002 M tellurium oxide (TeO_2). The ensuing CdTe thin-films were characterised using X-ray diffraction (XRD), UV-Vis spectrophotometry, scanning electron microscopy (SEM), energy dispersive X-ray (EDX) and photoelectrochemical (PEC) cell measurements. The electroplated CdTe thin-films exhibit a dominant (111) CdTe cubic structure, while the crystallite size increases with the increase in the electroplating temperature. The internal strain, dislocation density and the number of crystallites per unit area decrease with increasing growth temperature. The optical characterization depicts that the CdTe samples show comparable absorbance and a resulting bandgap of 1.51±0.03 eV for as-deposited CdTe layers. A marginal increase in the bandgap and reduction in the absorption edge slope towards lower deposition temperatures were also revealed. The annealed CdTe thin-films showed improvement in energy bandgap as it tends towards 1.45 eV while retaining the aforementioned absorption edge slope trend. Scanning electron microscopy shows that the underlying FTO layers are well covered with increasing grain size observable relative to the increase in the deposition temperature. The energy dispersive X-ray analyses show an alteration in the Te/Cd relative to the deposition temperature. Higher Te ratio with respect to Cd was revealed at deposition temperature lower than 85°C. The photoelectrochemical cell study shows that both *p*- and *n*-type CdTe can be electroplated and that deposition temperatures below 85°C at 1400 mV results in *p*-type CdTe layers.

Keywords: Electrodeposition; CdTe film; Two-electrode configuration; thin films, electroplating temperature

Introduction

Electrodeposition has emerged as a one of the versatile and cost-effective growth technique of metal, metalloid and semiconductor materials [1]. With emphasis on semiconductor growth, the use of either two- or three- electrode electroplating technique has been effective in the growth of high-performance semiconductor materials [2]. Asides the electroplating configuration, challenging factors affecting the reproducibility of electroplated materials include but not limited to the solutes, solvents, electrolytic bath ionic concentrations, solution aging (electroplating age) the stabilities of both growth pH and deposition temperature and the deposition current density [3]. Provided these factors are optimised, high-quality semiconductor materials such as cadmium telluride (CdTe) thin-films can be grown and incorporated for different applications. CdTe is one of the II-VI semiconductor materials that has been grown using several techniques including electroplating [4,5] and has been extensively researched owing to its properties [6]. Due to the direct bandgap of CdTe at room temperature (~1.45 eV), it is capable of absorbing a substantial fraction of the electromagnetic spectrum under AM1.5 condition. This characteristic has been explored in the photovoltaic (PV) community in achieving high-efficiency CdTe-based solar cells [7]. The recent hike in the conversion efficiency as reported in the literature is mainly due to the eradication of defects within the crystal lattice or traps within the bandgap in addition to improved crystallinity, passivation of the grain boundaries which is due to better understanding of both material and device issues. Therefore it is fundamental to strive towards process optimisation amongst others. Under both two and three- electrode electrodeposition configurations, different deposition temperatures have been utilised by independent researchers [8–14] without a unifying examination of the effect of electroplating temperature in aqueous solution. Although limiting factors such as reference electrode (with a functioning temperature less than 70°C) and the boiling temperature of water are to be reckoned with. Therefore, this publication examines the effect of temperature of the electrolyte on the structural, optical, morphological compositional properties and electronic properties of electrodeposited CdTe layers grown from an aqueous solution containing tellurium dioxide (TeO_2) and cadmium nitrate $Cd(NO_3)_2$ as the respective precursors of Te and Cd.

Materials and Methods

1.1   Thin-film synthesis

Cadmium telluride thin-films were electrodeposited from a solution containing 1.5 M cadmium nitrate tetrahydrate ($Cd(NO_3)_2 \cdot 4H_2O$) and 0.002 M tellurium oxide (TeO_2). The respective precursors for Cd and Te were dissolved in 400 ml of deionised (DI) water contained in a polypropylene beaker using the set up depicted in Figure 1. The resulting aqueous solution will be referred to as CdTe-bath henceforth in this report. Using these precursor concentrations and electrolytic cell set up, four electrolytic baths were created. To achieve a transparent and homogenous solution, the baths were stirred for about 300 min.
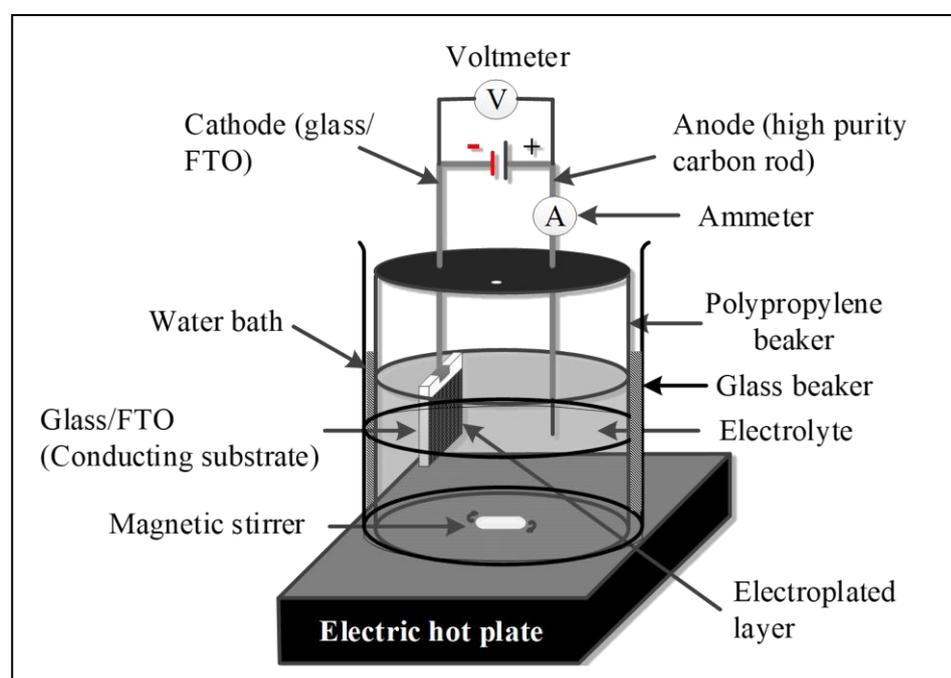

Figure 1: Typical two-electrode electrodeposition configuration.

Prior to electroplating, the pH and the magnetic stirring rate of the bath were maintained at 2.00 ± 0.02 and ~300 rpm. The adjustment of the pH is achieved by either using nitric (HNO_3) acid to lower the pH value or ammonium hydroxide (NH_4OH) – an alkaline to increase the pH value. The deposition temperature is set at 55°C, 65°C, 75°C, and 85°C for respective electrolytic baths, while the deposition voltage is kept constant at 1400 mV for all the CdTe layers. The 1400 mV cathodic growth voltage is based on prior optimisation of CdTe thin-films grown from a pure $Cd(NO_3)_2$ electrolyte as described in the literature [15]. The deposition temperature lower or higher than this range were not reported due to low adhesion of the ED-

CdTe thin-film and the formation of water bubbles on the g/FTO substrate due to the close proximity of the deposition temperature to the boiling point of water.

The glass/fluorine-doped tin oxide (g/FTO) substrates utilised as the working electrode were cut into strips with a dimension of 3×2 cm^2. The g/FTO strips were washed using soap water in an ultrasonic bath, alcohol, rinse thoroughly in DI water and dried using nitrogen gas [16]. After the thin-film layer deposition, the 3×2 cm^2 strips were cut in two halves of 3×1 cm^2 – one is left as-deposited (AD) while the other is cadmium chloride treated (CCT) to mimic the photovoltaic device-ready process. The CCT-CdTe layers were allowed to cool in the air before both the AD and the CCT layers were rinse to eliminate the loosely adhered particles of CdTe, Cd, and Te from the surfaces of the thin-film and dried in the presence of nitrogen gas.

It is necessary to note that cyclic voltammetry as shown in Figure 2 of the CdTe-bath was performed at electrolytic bath condition when bath temperature, pH, and stirring rate were set at 85°C, 2.00 ± 0.02 and ~300 rpm. The voltammogram is the current-voltage (I-V) curve of the CdTe-bath to determine the optimal cathodic voltage region for the deposition of CdTe.
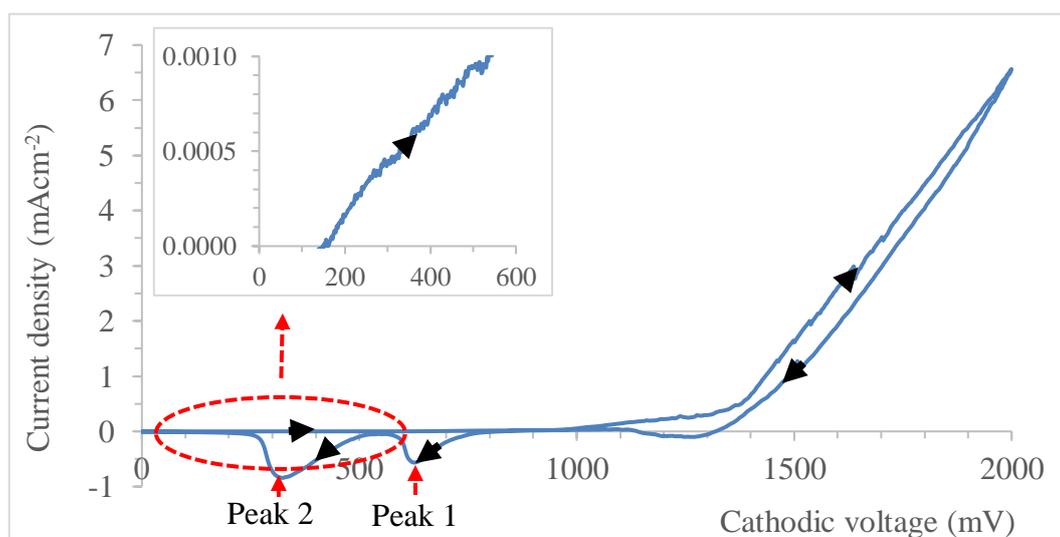

Figure 2: Typical cyclic voltammogram of an aqueous electrolyte at 85 °C containing 1.5 M Cd(NO$_3$)$_2$·4H$_2$O and 0.0002 M TeO$_2$ in 400 ml of DI water.

Tellurium is deposited first because it is more positive as compared to cadmium with respective standard reduction potential value of +593 mV and -403 mV with respect to standard H$_2$ electrode. From the inset of Figure 2, Te starts depositing at a cathodic voltage of ~170 mV and above, while Cd starts deposition at 1000 mV. Details of the optimisation process have been documented by the author's group in the literature [10,15].

4

1.2   Thin-film characterisation

The structural characterisation was carried out using Philips PW 3,710 X'pert diffractometer mounted with 1.5406 Å wavelength Cu-Kα monochromator. The X-ray diffraction system is also equipped with X'Pert High Score which aided with phase identification, dominant diffraction and for the estimation of the crystallite sizes. For the experiments presented in this work, thin-films were scanned between the range of 2θ=(20 and 70)°. Using the Scherrer formula as shown in Equation 1, the crystallite size D was estimated. Where β denotes the full-width-at-half-maximum (FWHM) of the diffraction intensity in radians, θ denotes the Bragg angle, λ denotes the X-rays wavelength (which is 1.5406 Å for Cu-Kα monochromator) and K is the shape constant. For spherical geometry, K is taken as 0.94.

$$D = \frac{K\lambda}{\beta \cos \theta} \qquad \text{Equation 1}$$

The internal micro-strain, ε, which defines the crystallites distortion due to tensile or compressive stress is calculated for the thin-films using Equation 2 as documented in Ref [17].

$$\varepsilon = \frac{\beta}{4 \tan \theta} \qquad \text{Equation 2}$$

The dislocation density, δ, which defines the length of dislocation lines per unit volume of crystal in the thin-film is calculated using Equation 3 as reported in the literature [18]

$$\delta = \frac{1}{D^2} \qquad \text{Equation 3}$$

The estimation of the number of crystallites per unit area in the thin-film, N, was done using Equation 4 as documented in Ref [18,19].

$$N = \frac{t}{D^3} \qquad \text{Equation 4}$$

The film thickness was measured using a UBM Microfocus optical profilometer and mathematically estimated using Faraday's law of electrolysis (see Equation 5), where T is the film thickness, J is the average current density during deposition, M is the molar mass of CdTe (M_{CdTe}=240.01 gmol^{-1}), t is the duration of deposition, n is the number of electrons transferred for deposition of 1 molecule of CdTe (n=6), and F is the constant defined by Faraday as 96485 Cmol^{-1}, and ρ is the density of CdTe.

$$T = \frac{JMt}{n\rho F} \qquad \text{Equation 5}$$

The optical absorbance data of the electroplated thin-films were taking within the range of 200 nm to 800 nm using Cary50 Scan UV-visible spectrophotometer. From the absorbance data accumulated within the specified wavelength range, the bandgap was estimated using the Tauc's formula illustrated in Equation 6 via the graph of $(\alpha h v)^2$ versus $(h v)$. Where the coefficient of absorption is represented by α, the bandgap energy is represented by E_g, the Planck's constant is represented by h, the incident photon frequency is represented by v, the proportionality constant which depends on the refractive index of the sample under investigation is represented by k, and m equals 0.5 for a direct bandgap semiconductor. The extrapolation of the straight line portion of the Tauc's plot (at $(\alpha h v)^2=0$) gives the bandgap energy.

$$\alpha = \frac{k\left(h v - E_g\right)^m}{h v} \qquad \text{Equation 6}$$

The examination of the thin film's surface morphology and composition was performed in vacuum condition using FEI Nova200 NanoSEM fitted with energy dispersive X-ray (EDX) detector. The confirmation of the electrical conduction type is done using photoelectrochemical (PEC) cell measurements by the formation of a junction between the solid (g/FTO/CdTe) and liquid (an aqueous solution of 0.1 M $Na_2S_2O_3$ in 20 ml DI water). The comprehensive detail of the PEC set up is incorporated in Ref [16].

Result and discussion

1.3   Material characterisation

In order to validate the results in this Section, all the stated values correspond to the average of three replica samples investigated under the same conditions.

1.3.1   X-ray diffraction (XRD) analysis

For this set of experiments, the thicknesses of the CdTe layers electrodeposited at a different temperature from CdTe-baths was maintained at ~1µm under as-deposited condition using factors such as deposition time, stirring rate amongst others. Figure 3 (a) and Figure 3 (b) illustrate the typical XRD patterns of CdTe thin-films electrodeposited at different growth temperature under as-deposited (AD) and cadmium chloride treated (CCT) conditions respectively. While Table 1 and Table 2 is the respective summaries of the X-ray diffraction analysis for cubic (111) CdTe diffraction for AD and CCT-CdTe layers and the comparative analysis of strain, dislocation density and number of crystallites per unit area of the CdTe thin-

films electroplated at a different temperature. Under both the AD and CCT conditions, the CdTe layers show diffraction patterns with a preferential and strong (111) phase of the cubic structure of CdTe at $2\theta = \sim24.0°$ (see Figure 3 (a) and Figure 3 (b)). This is asides the diffractions at $2\theta = \sim20.6°$, $\sim33.8°$, $\sim37.9°$, $\sim51.6°$, $\sim60.7°$ and $\sim65.6°$ associable with the underlying g/FTO substrate. This is in addition to the cadmium tellurate (Cd_xTeO_y) diffraction observed at $2\theta = 23.0°$. With respect to the AD-CdTe layers shown in Figure 3 (a) and Table 1, an increase in the deposition temperature resulted in an increase in the cubic (111) CdTe diffraction intensity, peak sharpness, and crystallite size as evident by the 65.8 nm observed at 85°C. This indicates an enhancement in the crystallinity and a reduction in the lattice defects of the CdTe-layers at high deposition temperature. This observation can also be said of the CCT-CdTe layers with the highest cubic (111) CdTe intensity at 85°C (see Figure 3 (b) and Table 1).
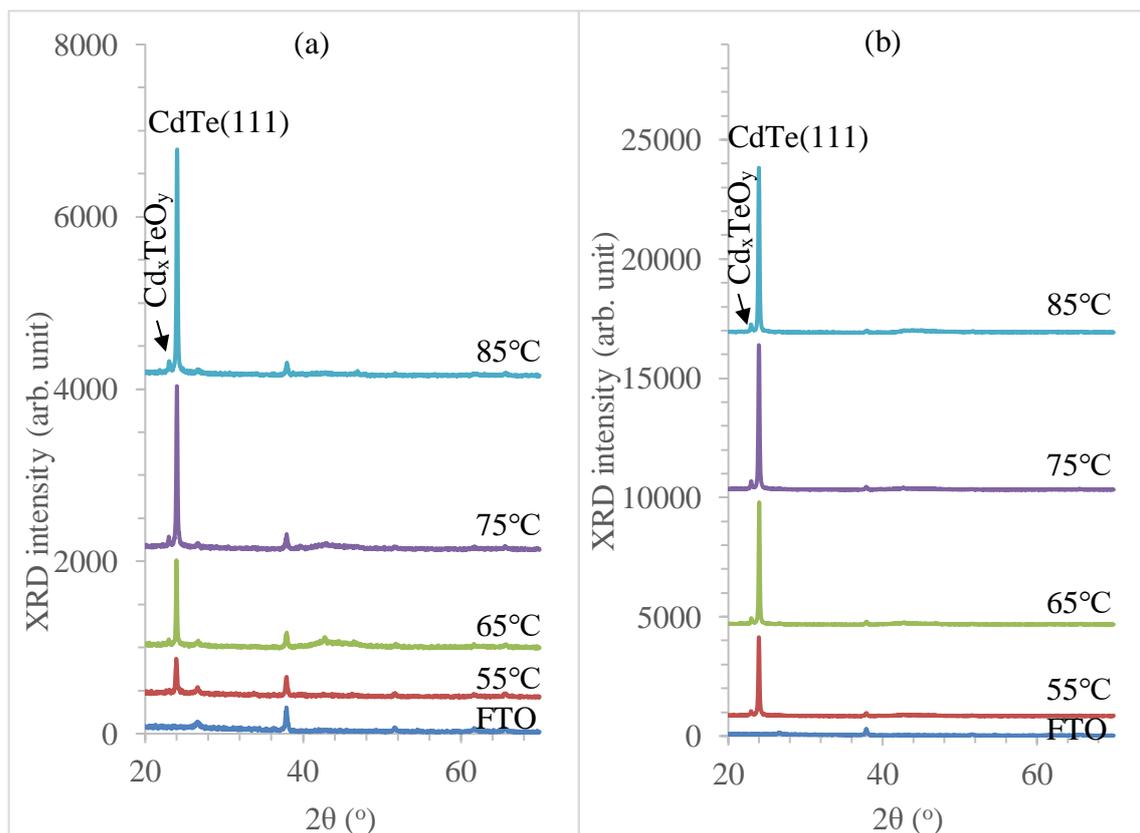

Figure 3: XRD patterns of CdTe thin-films electroplated at different temperatures under (a) AD and (b) CCT conditions.

With emphasis on the CdTe (111)C preferred orientation, a drastic improvement in the intensity of the diffraction after CCT treatment and crystallite size was observed notwithstanding the CdTe-bath deposition temperature. Interestingly, a reduction in the micro-strain, the dislocation density and the number of crystallites per unit area was observed with an increase in the deposition temperature, while further improvements were observed even after CCT (see Table 2 and Figure 4). This observations might be as a result of the recrystallization of the polycrystalline CdTe thin-films during treatment which results to the improvement in the Cd/Te stoichiometry by the sublimation of surplus elements or the formation of CdTe by the reaction between surplus elemental Te and Cd from $CdCl_2$ treatment [4,22]. It should be noted that no matter the deposition technique, Te –precipitation is one of the main challenges in the deposition of CdTe [23,24]

Table 1: Summary of the X-ray diffraction analysis for cubic (111) CdTe diffraction for AD and CCT-CdTe layers

Deposition temperature ($\pm 2°C$)	2θ (°)	Lattice spacing (Å)	FWHM (°)	Crystallite size D (nm)	Micro-strain $\varepsilon_1 \times 10^{-3}$	Dislocation density $\delta_1 \times 10^{11}$ (lines•cm^{-2})	Number of crystallites per unit area N_1 $\times 10^{12}$ (cm^{-2})
AD							
55	23.9	3.73	0.227	37.4	4.68	7.15	1.91
65	23.8	3.74	0.195	43.5	4.04	5.28	1.21
75	23.9	3.72	0.162	52.4	3.33	3.64	0.69
85	24.0	3.70	0.129	65.8	2.64	2.31	0.35
CCT							
55	23.9	3.714	0.162	52.4	3.33	3.64	0.69
65	24.0	3.708	0.129	65.8	2.65	2.31	0.35
75	24.0	3.713	0.129	65.8	2.65	2.31	0.35
85	24.0	3.715	0.129	65.8	2.65	2.31	0.35

Improvement in the crystallinity of CdTe after post-growth treatment in the presence of chlorine due to factors such as grain growth, recrystallization amongst others is generally accepted by the scientific community [25,26]. The stagnation observed in the crystallite size at 65.8 nm might be as a result of the limitation of the XRD machine utilised and/or that of the Scherrer's formula utilised in the measurement and analysis of CdTe thin-films respectively [27,28].

Table 2: Comparative analysis of strain, dislocation density and number of crystallites per unit area of the CdTe films electroplated at different temperature under AD and CCT conditions.

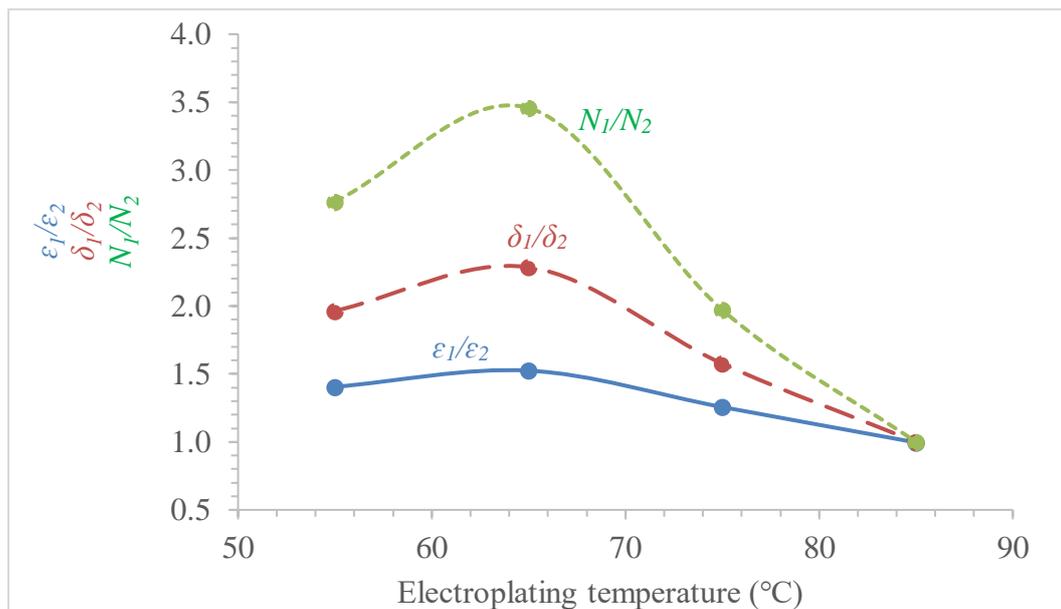| Deposition temperature (±2°C)	$\varepsilon_1/\varepsilon_2$	δ_1/δ_2	N_1/N_2
55	1.41	1.96	2.77
65	1.52	2.29	3.46
75	1.26	1.58	1.97
85	1.00	1.00	1.00

Figure 4: Comparative analysis of strain, dislocation density and Number of crystallites per unit area of the CdTe films electroplated at different cathodic voltages.

The obtained XRD diffraction data from the CdTe thin film structural analysis is in agreement with the 01-075-2086 reference file of the Joint Committee on Powder Diffraction Standards (JCPDS) for cubic CdTe layers.

1.3.2 Thickness measurement

For this experiment, the deposition duration was maintained at 180 min for each of the electroplated CdTe at different deposition temperatures. Figure 5 shows the graphical plot of both the estimated and the measured thicknesses including the average deposition current density of the CdTe layers against the deposition temperature. For the estimated thickness using the Faraday's equation (see Equation 5), the rise in the thickness of electrodeposited CdTe with increasing deposition temperature was solely due to the corresponding increase in the average current density of deposition. The increase in the deposition temperature increases the mobility

of the molecules and constituent ions within the electrolyte and also increases the solubility of the solvent and catalyses the reactions. Correspondingly, this divulges to an increase in the deposition current density and hence, a rapid growth rate of constituent elements or compounds.

The observed deviation of the estimated thickness and the measured thickness is due to the assumption that all the electronic charges flowing through electrolytic cell partake in the growth of the electroplated materials made by Faraday's law of electrolysis. The assumption did not consider the electronic charges associated with the breakdown of water into its constituent ions. Therefore, the estimated thickness using Faraday's formula served as the upper limit of the thickness. Based on observation, a greater deviation between the measured and the estimated thickness was observed for the CdTe layers grown at 85°C. Due to the favourable impact higher temperature to molecular and ionic activity within the electrolyte.
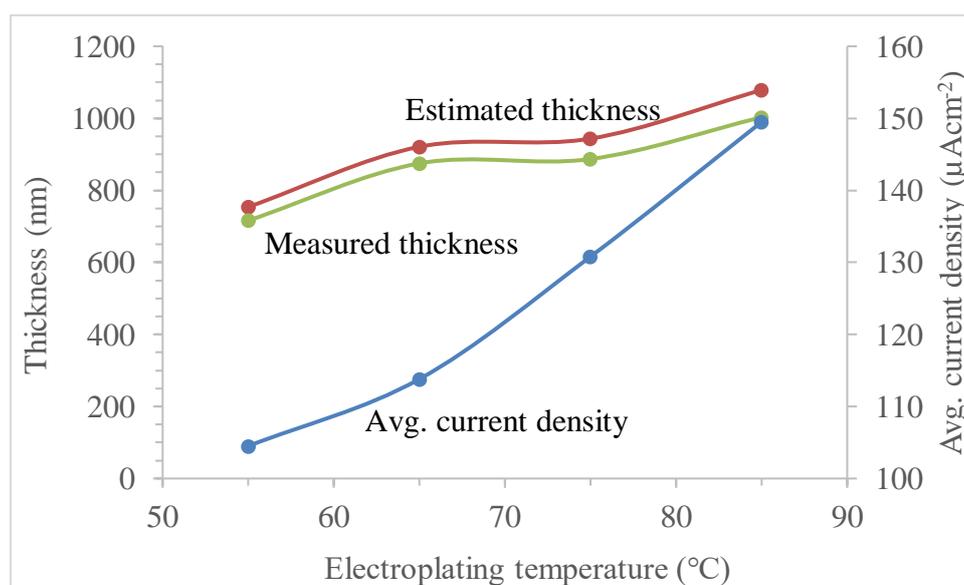

Figure 5: A plot of the estimated and measured thicknesses (as-deposited) and the average current density during electroplating against the electroplating temperature for CdTe layers grown for 180 minutes.

1.3.3   Optical properties analysis

Figure 6 (a) and Figure 6 (b) shows the Tauc's plot of $(\alpha h v)^2$ against $(h v)$ for CdTe thin-films electrodeposited at different temperatures under both AD and CCT conditions respectively. Table 3 and Figure 7 summarises the observed bandgap energy and the absorption edge of the

investigated CdTe thin-films. Under the as-deposited condition, the observed bandgaps range is within the generally acceptable range of 1.51±0.03 eV for CdTe layers [29]. This follows a trend in which the highest bandgap of 1.54 eV was recorded at 55°C and the lowest bandgap of 1.48 eV was observed at 85°C. It is generally accepted in the photovoltaic community that the optimal bandgap 1.45 eV is required to achieve the highest efficiency of a one-bandgap *p-n* junction photovoltaic device.
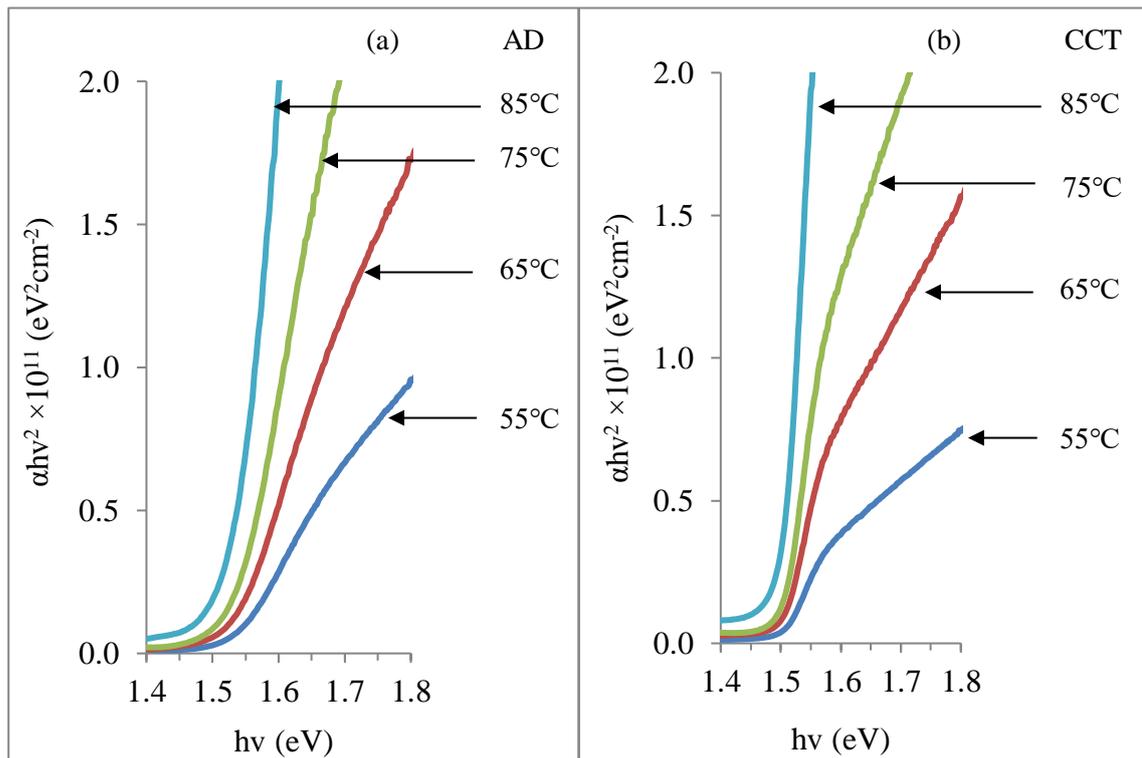

Figure 6: Optical absorption spectra for electroplated CdTe thin-films electroplated at different deposition temperature under (a) AD and (b) CCT conditions.

A shift towards 1.45 eV bandgap was observed after post-growth treatment –CCT as shown in Figure 6 (b), Figure 7 and Table 3. This observation should be as a result of the improvement in the characteristic properties of CdTe [25,26]. Further to this, a shift in the absorption edge slope was also observable, with the highest edge slope observed at 85°C under both AD and CCT conditions. It is known that the sharpness of the absorption edge slope indicates lesser impurity energy levels and defects in the thin-films under investigation [4,30,31]. This observation suggests that more stoichiometric CdTe layers are deposited at 85°C and a further improvement is achievable after CCT. This observation is in agreement with the summation made in Section 1.3.1.

Table 3: The optical bandgap and absorption edge slope of CdTe layers electroplated from electrolytes at different temperatures

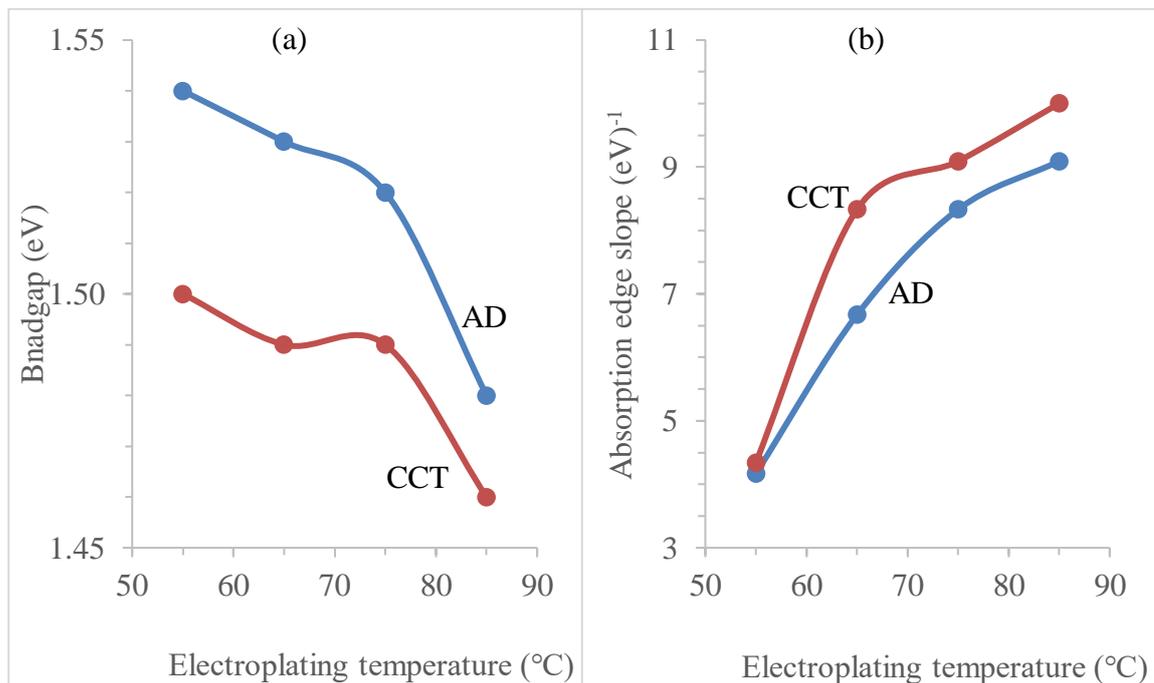| Electroplating temperature (°C)	Bandgap (eV)		Abs. edge slope (eV^{-1})	
	AD	CCT	AD	CCT
55	1.54	1.50	4.17	4.34
65	1.53	1.49	6.67	8.33
75	1.52	1.49	8.33	9.09
85	1.48	1.46	9.09	10.00

Figure 7: (a) A plot of optical bandgap of CdTe electroplated from electrolytes at different deposition temperature and (b) is the absorption edge slope of the CdTe layers under both AD and CCT conditions against deposition temperature.

1.3.4 Morphological properties analysis

Figure 8 (a) to Figure 8 (d) shows the SEM images of CCT-CdTe thin-films electrodeposited at different growth temperatures ranging for 55°C to 85°C. The CdTe thin-films deposited at all the explored deposition temperatures show excellent coverage of the underlying g/FTO substrate. The purported good coverage is due to the good quality of the CdTe layers deposited based on the electrodeposition parameters such as the cathodic voltage, stirring rate, pH amongst other factors prior to CCT. While the retention of the complete coverage after CCT is

owing to the enhancements in the CdTe micro-structure as a result of the recrystallization, sublimation of superfluous elements, grain growth and the formation of CdTe via a chemical reaction between excess Cd from $CdCl_2$ and precipitated Te in the layer. In AD-CdTe, cauliflower-like clusters consisting of numerous crystals are often observed with sizes ranging between ~(30 and 65) nm [15]. Upon CCT, these crystals merge into grains due to their large surface to volume ratio. This is a key feature of nano-materials and helps in the formation of large grains. The CCT-CdTe grains are much larger with grains sizes ranging between ~(200 and 6000) nm.
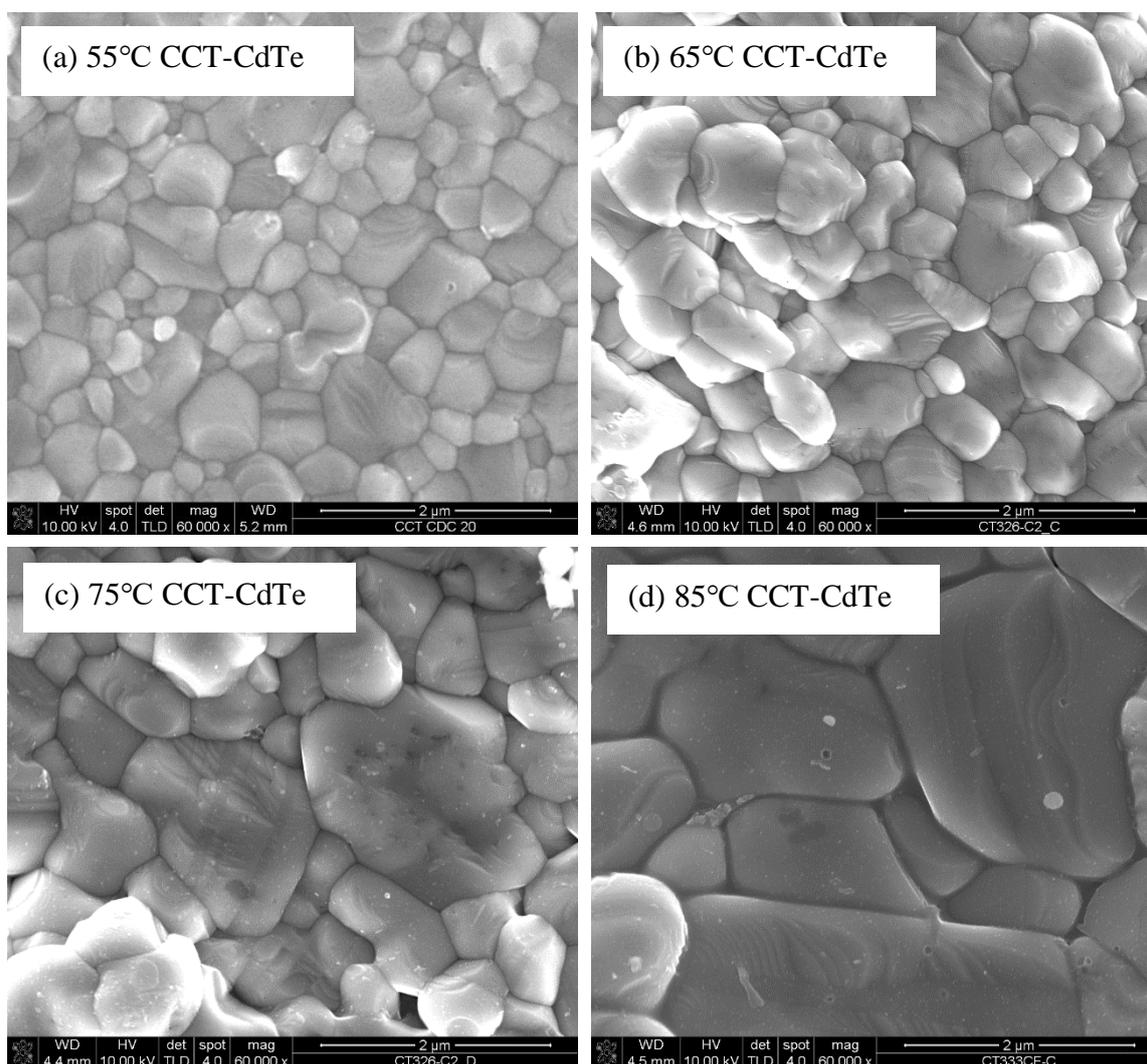

Figure 8: Typical 2-dimensional SEM micrographs for $CdCl_2$ treated CdTe samples grown from electrolyte at different electroplating temperature between 55°C and 85°C.

Based on topological observation, a gradual increase in the grain size with increasing deposition temperature was noted with the largest grain size of 6 µm and lower grain boundary density observed for the 85°C bath. This observation indicates that although CCT facilitates

grain growth in CdTe, high deposition temperature favours grain growth. It is relevant at this point to compare the noted trend of the grain size in Figure 8 with the deductions made based on the number of crystallites per unit area N_I in Section 1.3.1. It is at this point important to note that the calculated crystallite size using the Scherrer formula in XRD analysis does not translate to the sizes of grains observed in the SEM micrograph, nonetheless, the grains are formed from many crystallites.

1.3.5 Compositional measurement

Figure 9 shows the typical EDX spectra for AD and CCT-CdTe grain at 85℃ and the plot of the atomic composition ratio of Te to Cd in electroplated CdTe layers under both AD and CCT conditions against the electroplating temperature. Asides from Te and Cd elements, other elements such as O, F, Sn, Si were also randomly observed owing to layer oxidation and/or the underlying g/FTO substrate. With emphasis on the as-deposited CdTe layers as shown in Figure 9, the compositional ratio of Te/Cd is less than 1 for the CdTe thin-film deposited at 85℃. The CdTe thin-films grown at deposition temperature 75℃ and below show comparative Te-richness.

It can be recalled from the succinct discussion on the cyclic voltammogram in Section 1.1 and Figure 2, there seems to be continued shift in the graph to the right with decreasing deposition temperature resulting. This argument is valid due to the catalytic effect of heat in reaction and in the mobility of ions constituted in the electrolyte especially Cd with comparatively lower redox potential. This is one of the possible reasons for the Cd or Te richness of the deposited CdTe layer at the same cathodic voltage at the exploring temperature of 85℃ and between (55 and 85)℃ respectively. After CCT, a shift towards stoichiometry in the atomic composition ratio of the CdTe layers was observed (see Figure 9). Which might be influenced by the reaction between Cd from $CdCl_2$ with unreacted Te and/or the sublimation of excess elemental Cd and Te from the layer. For photovoltaic applications, the richness of Cd in CdTe used as an absorber layer has been documented in the literature to produce a comparatively higher efficiency [32–35]. A stoichiometry of 50/50 Te to Cd atomic composition was observed for the 85℃ CdTe after CCT signify comparatively higher crystallinity. This observation is in agreement with the high crystallinity level observed at 85℃.
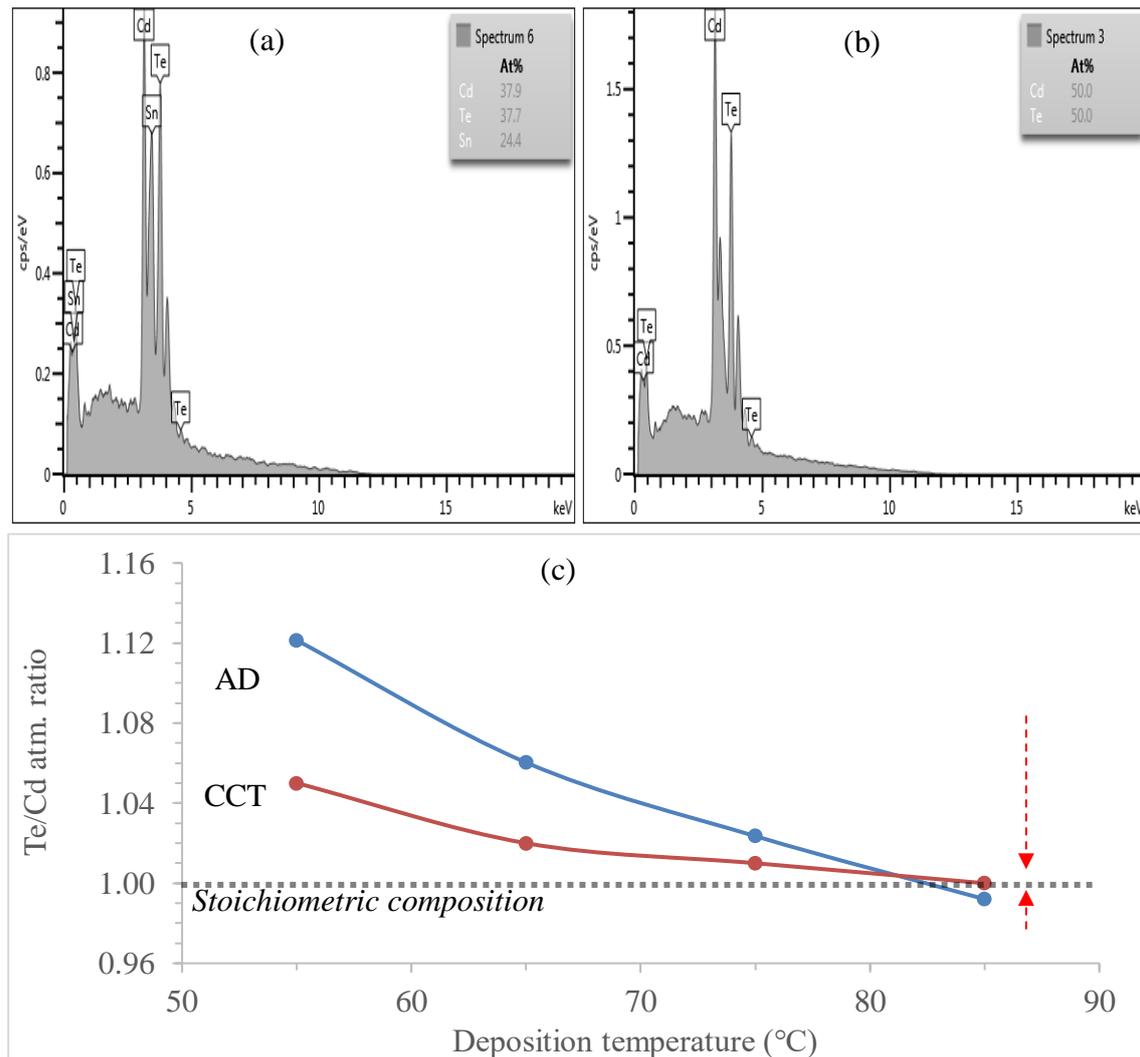
Figure 9: EDX spectra of CdTe grown from the 85°C electrolyte under (a) AD, (b) CCT conditions (c) is the graphical summary of Te/Cd atomic composition ratio against electroplating temperature of CdTe for both AD and CCT samples.

1.3.6   Photoelectrochemical (PEC) cell measurement

Figure 10 shows the PEC cell measurements of the CdTe layers electroplated from electrolytes at different deposition temperature against electroplating temperature under both AD and CCT conditions. An all-round technique such as the Hall-Effect measurement was not used because of the effect of the highly conductive FTO underlying substrate. The obtained data cannot be isolated only for CdTe from the measurement.
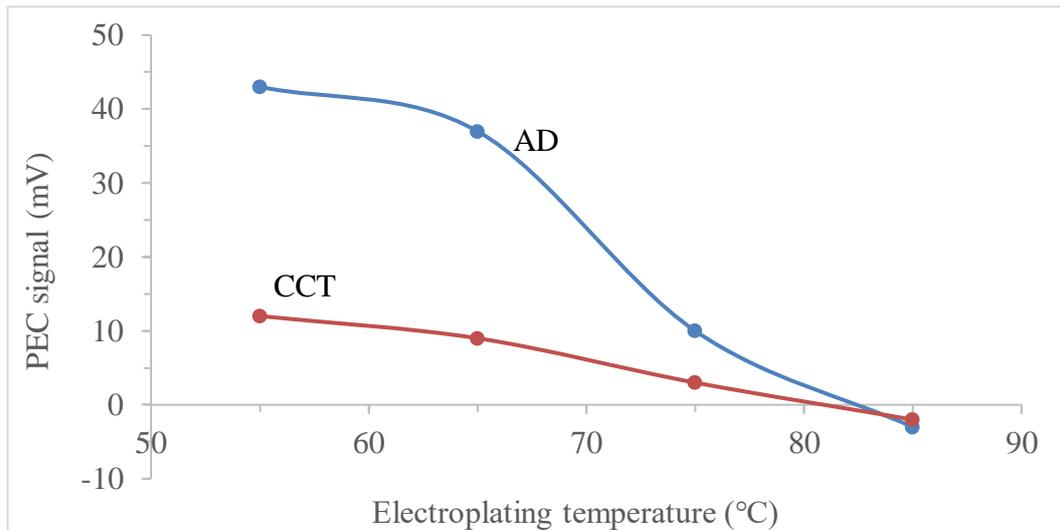
Figure 10: A plot of PEC signal of CdTe electroplated from electrolytes at different deposition temperatures against electroplating temperature under both AD and CCT conditions.

As depicted in Figure 10, the electrical conduction type of the as-deposited CdTe layers grown at 85°C is *n*-type while the ones grown at between (55 and 75)°C are *p*-type. A similar observation is also been made of the CdTe layers after CCT with a shift from the *n*-type layers towards p-type electrical conductivity and vice versa, while the initial conduction types were retained. The observed PEC signal shift after CCT is an attribute of recrystallization amongst factors that have been well document [25,26]. It is captivating that the observed PEC trend is somewhat similar to that of the EDX spectra summary in Figure 9 (c). This is because one of the predominant factors determining the electrical conduction type is the atomic compositional ratio of the constituent elements, with Te-richness in CdTe resulting in p-type and Cd-richness resulting in *n*-type conduction type [16,32,33]. Other factors include the heat treatment parameters (such as duration, temperature), preliminary atomic composition of Cd and Te, the concentration of $CdCl_2$ or other dopants utilised in treatment, the structure of the defects in the material, and the initial conductivity type of the material. [8,15,25,36].

Conclusions

The effect of deposition temperature in a two-electrode electrodeposition configuration was explored and the ensued CdTe thin-films were methodically characterised and presented. The structural, optical, morphological, compositional, and electronic properties of the CdTe relative to their deposition temperature was studied. All the electroplated thin-films grown at a different

deposition temperature of the electrolyte show polycrystalline cubic structure of the material with a preferred orientation along the (111) plane. A perusal of the structural properties depicts that CdTe crystallites of the electrodeposited thin-films are less strained with increasing deposition temperature with internal strain values of 4.68×10^{-3} for the CdTe deposited at 55°C and 2.64×10^{-3} for the grown CdTe at 85°C. These values were reduced after post-growth CCT. The dislocation density for the as-deposited CdTe was observed to be 7.15×10^{11} lines•cm^{-2} for the CdTe deposited at 55°C and 2.31×10^{11} lines•cm^{-2} for the grown CdTe at 85°C, which was respectively reduced to 3.64 and 2.31 lines•cm^{-2}. The number of crystallites per unit area N was found to reduce from $(1.91 \times 10^{12}$ to $0.35 \times 10^{12})$ cm^{-2} with increased deposition temperature from (55 to 85)°C. The N was found to reduce to $(0.69 \times 10^{12}$ to $0.35 \times 10^{12})$ cm^{-2} with increased deposition temperature from (55 to 85)°C after CCT. This is an indication that the crystallite sizes increases after annealing. This was evident with the crystallite sizes of the as-deposited films ranging from (37.4 to 65.8) nm with increased deposition temperature from (55 to 85)°C to (52.4 to 65.8) nm after post-growth CCT. The optical property investigation reveals that, the deposited layers possess bandgaps ranging between 1.51±0.03 eV under as-deposited condition and 1.48±0.02 eV after CCT. Prominently, the sharpness of the optical absorption edge slope reduces with the reduction in the deposition temperature. Morphologically, all the electrodeposited layers show full underlying layer coverage. Comparatively, larger grains after CCT was observed for layers grown at 85°C. The compositional analysis reveal that Cd and Te are presence in the deposited thin-film. A ratio of 1:1 was recorded for CdTe layers grown at electroplating temperature of 85°C, but an increase in the atomic concentration of Te with the reduction of the electroplating temperature from (85 to 55)°C was noted. The PEC measurements show that the CdTe layers grown at 85°C is *n*-type under both AD and CCT conditions, while p-type conduction type CdTe layers ensued for the layers grown at deposition temperature of 75°C and below. These results underline the importance of the deposition temperature in the electrodeposition and the capability of two-electrode electrodeposition configuration. Asides the elimination of possible contaminants from the reference electrode in this configuration, 2-electrode system also provides the leeway of electroplating at higher temperatures to improve the material and electronic qualities of PV materials.

Conflict of interest

We have no conflicting interest.

References

[1]   D. Lincot, Electrodeposition of semiconductors, Thin Solid Films. 487 (2005) 40–48. doi:10.1016/j.tsf.2005.01.032.

[2]   I. Dharmadasa, M. Madugu, O. Olusola, O. Echendu, F. Fauzi, D. Diso, A. Weerasinghe, T. Druffel, R. Dharmadasa, B. Lavery, J. Jasinski, T. Krentsel, G. Sumanasekera, Electroplating of CdTe Thin Films from Cadmium Sulphate Precursor and Comparison of Layers Grown by 3-Electrode and 2-Electrode Systems, Coatings. 7 (2017) 17. doi:10.3390/coatings7020017.

[3]   A.A. Ojo, I.M. Dharmadasa, Electroplating of Semiconductor Materials for Applications in Large Area Electronics: A Review, Coatings. 8 (2018) 262. doi:10.3390/coatings8080262.

[4]   A. Bosio, N. Romeo, S. Mazzamuto, V. Canevari, Polycrystalline CdTe thin films for photovoltaic applications, Prog. Cryst. Growth Charact. Mater. 52 (2006) 247–279. doi:10.1016/j.pcrysgrow.2006.09.001.

[5]   A.K. Turner, J.M. Woodcock, M.E. Özsan, D.W. Cunningham, D.R. Johnson, R.J. Marshall, N.B. Mason, S. Oktik, M.H. Patterson, S.J. Ransome, BP solar thin film CdTe photovoltaic technology, Sol. Energy Mater. Sol. Cells. 35 (1994) 263–270. doi:10.1016/0927-0248(94)90149-X.

[6]   B.E. McCandless, J.R. Sites, Cadmium Telluride Solar Cells, in: Handb. Photovolt. Sci. Eng., John Wiley & Sons, Ltd, Chichester, UK, 2005: pp. 617–662. doi:10.1002/0470014008.ch14.

[7]   M.A. Green, Y. Hishikawa, E.D. Dunlop, D.H. Levi, J. Hohl-Ebinger, A.W.Y. Ho-Baillie, Solar cell efficiency tables (version 51), Prog. Photovoltaics Res. Appl. 26 (2018) 3–12. doi:10.1002/pip.2978.

[8]   N.A. Abdul-Manaf, H.I. Salim, M.L. Madugu, O.I. Olusola, I.M. Dharmadasa, Electro-Plating and Characterisation of CdTe Thin Films Using CdCl2 as the Cadmium Source, Energies. 8 (2015) 10883–10903. doi:10.3390/en81010883.

[9]   O.K. Echendu, K.B. Okeoma, C.I. Oriaku, I.M. Dharmadasa, Electrochemical Deposition of CdTe Semiconductor Thin Films for Solar Cell Application Using Two-Electrode and Three-Electrode Configurations: A Comparative Study, Adv. Mater. Sci. Eng. 2016 (2016) 1–8. doi:10.1155/2016/3581725.

[10]   A.A. Ojo, W.M. Cranton, I.M. Dharmadasa, CdTe Deposition and Characterisation, in: Next Gener. Multilayer Graded Bandgap Sol. Cells, Springer International Publishing, Cham, 2019: pp. 123–183. doi:10.1007/978-3-319-96667-0_6.

[11]   H. Gómez, R. Henríquez, R. Schrebler, R. Córdova, D. Ramírez, G. Riveros, E. a. Dalchiele, Electrodeposition of CdTe thin films onto n-Si(100): nucleation and growth mechanisms, Electrochim. Acta. 50 (2005) 1299–1305. doi:10.1016/j.electacta.2004.08.020.

[12]   K. Murase, T. Honda, M. Yamamoto, T. Hirato, Y. Awakura, Electrodeposition of CdTe from Basic Aqueous Solutions Containing Ethylenediamine, J. Electrochem. Soc. 148 (2001) C203. doi:10.1149/1.1348259.

[13]   S.K. Das, G.C. Morris, Influence of growth and microstructure of electrodeposited cadmium telluride films on the properties of n -CdS/ p -CdTe thin-film solar cells, J. Appl. Phys. 72 (1992) 4940–4945. doi:10.1063/1.352062.

[14]   K.D.M.S.P.K. Kumarasinghe, D.S.M. De Silva, K.A.S. Pathiratne, H.I. Salim, N.A. Abdul-Manaf, I.M. Dharmadasa, Electrodeposition and characterization of as-deposited and annealed CdTe thin films, Ceylon J. Sci. 45 (2016) 53. doi:10.4038/cjs.v45i2.7388.

[15]   H.I. Salim, V. Patel, a. Abbas, J.M. Walls, I.M. Dharmadasa, Electrodeposition of CdTe thin films using nitrate precursor for applications in solar cells, J. Mater. Sci. Mater. Electron. 26 (2015) 3119–3128. doi:10.1007/s10854-015-2805-x.

[16]   A.A. Ojo, W.M. Cranton, I.M. Dharmadasa, Next Generation Multilayer Graded Bandgap Solar Cells, Springer International Publishing, Cham, 2019. doi:10.1007/978-3-319-96667-0.

[17]   G.K. Williamson, W.H. Hall, X-ray line broadening from filed aluminium and wolfram, Acta Metall. 1 (1953) 22–31. doi:10.1016/0001-6160(53)90006-6.

[18]   G.K. Williamson, R.E. Smallman, Dislocation densities in some annealed and cold-worked metals from measurements on the X-ray debye-scherrer spectrum, Philos. Mag. 1 (1956) 34–46. doi:10.1080/14786435608238074.

[19]   S. Prabahar, M. Dhanam, CdS thin films from two different chemical baths - Structural and optical analysis, J. Cryst. Growth. 285 (2005) 41–48. doi:10.1016/j.jcrysgro.2005.08.008.

[20]   A.C. Rastogi, K.S. Balakrishnan, Growth, Structure and Composition of Electrodeposited CdTe Thin Films for Solar Cells, Sol. Energy Mater. Sol. Cells. 36 (1995) 121–146. doi:10.1016/0927-0248(94)00167-Q.

[21]   P. Fernández, Defect structure and luminescence properties of CdTe based compounds, J. Optoelectron. Adv. Mater. 5 (2003) 369–388.

[22]   I.M. Dharmadasa, O.K. Echendu, F. Fauzi, N.A. Abdul-Manaf, O.I. Olusola, H.I. Salim, M.L. Madugu, A.A. Ojo, Improvement of composition of CdTe thin films during heat

treatment in the presence of CdCl2, J. Mater. Sci. Mater. Electron. 28 (2017) 2343–2352. doi:10.1007/s10854-016-5802-9.

[23]   J.C. Tranchart, P. Bach, A gas bearing system for the growth of CdTe, J. Cryst. Growth. 32 (1976) 8–12. doi:10.1016/0022-0248(76)90003-8.

[24]   N.V. V Sochinskii, V.N.N. Babentsov, N.I.I. Tarbaev, M.D. Serrano, E. Dieguez, The low temperature annealing of p-cadmium telluride in gallium-bath, Mater. Res. Bull. 28 (1993) 1061–1066. doi:http://dx.doi.org/10.1016/0025-5408(93)90144-3.

[25]   I.M. Dharmadasa, Review of the CdCl2 Treatment Used in CdS/CdTe Thin Film Solar Cell Development and New Evidence towards Improved Understanding, Coatings. 4 (2014) 282–307. doi:10.3390/coatings4020282.

[26]   A. Bosio, G. Rosa, D. Menossi, N. Romeo, How the Chlorine Treatment and the Stoichiometry Influences the Grain Boundary Passivation in Polycrystalline CdTe Thin Films, Energies. 9 (2016) 254. doi:10.3390/en9040254.

[27]   A. Monshi, Modified Scherrer Equation to Estimate More Accurately Nano-Crystallite Size Using XRD, World J. Nano Sci. Eng. 02 (2012) 154–160. doi:10.4236/wjnse.2012.23020.

[28]   A. Bouraiou, M.S. Aida, O. Meglali, N. Attaf, Potential effect on the properties of CuInSe2 thin films deposited using two-electrode system, Curr. Appl. Phys. 11 (2011) 1173–1178. doi:10.1016/j.cap.2011.02.014.

[29]   S.M. Sze, K.K. Ng, Physics of Semiconductor Devices, John Wiley & Sons, Inc., Hoboken, NJ, USA, 2006. doi:10.1002/0470068329.

[30]   J. Han, C. Spanheimer, G. Haindl, G. Fu, V. Krishnakumar, J. Schaffner, C. Fan, K. Zhao, a. Klein, W. Jaegermann, Optimized chemical bath deposited CdS layers for the improvement of CdTe solar cells, Sol. Energy Mater. Sol. Cells. 95 (2011) 816–820. doi:10.1016/j.solmat.2010.10.027.

[31]   D.T.F. Marple, Optical absorption edge in CdTe: Experimental, Phys. Rev. 150 (1966) 728–734. doi:10.1103/PhysRev.150.728.

[32]   M.O. Reese, C.L. Perkins, J.M. Burst, S. Farrell, T.M. Barnes, S.W. Johnston, D. Kuciauskas, T.A. Gessert, W.K. Metzger, Intrinsic surface passivation of CdTe, J. Appl. Phys. 118 (2015) 155305. doi:10.1063/1.4933186.

[33]   J.M. Burst, J.N. Duenow, D.S. Albin, E. Colegrove, M.O. Reese, J.A. Aguiar, C.-S. Jiang, M.K. Patel, M.M. Al-Jassim, D. Kuciauskas, S. Swain, T. Ablekim, K.G. Lynn, W.K. Metzger, CdTe solar cells with open-circuit voltage breaking the 1 V barrier, Nat. Energy. 1 (2016) 16015. doi:10.1038/nenergy.2016.15.

[34]   D.G. Diso, F. Fauzi, O.K. Echendu, O.I. Olusola, I.M. Dharmadasa, Optimisation of CdTe electrodeposition voltage for development of CdS/CdTe solar cells, J. Mater. Sci. Mater. Electron. 27 (2016) 12464–12472. doi:10.1007/s10854-016-4844-3.

[35]   I.M. Dharmadasa, A.A. Ojo, Unravelling complex nature of CdS/CdTe based thin film solar cells, J. Mater. Sci. Mater. Electron. 28 (2017) 16598–16617. doi:10.1007/s10854-017-7615-x.

[36]   B.M. Basol, Processing high efficiency CdTe solar cells, Int. J. Sol. Energy. 12 (1992) 25–35. doi:10.1080/01425919208909748.